JOURNAL OF GEOPHYSICAL RESEARCH, VOL. 101, NO. D14, PAGES 19,299–19,318, AUGUST 27,1996

# Aerosol optical depth over Canada and the link with synoptic air mass types

**A.** Smirnov, N.T. O'Neill, A. Royer, and A. Tarussov

Centre d'Applications et de Recherches en Télédétection, Université de Sherbrooke, Sherbrooke, Quebec, Canada

B. McArthur

Experimental Studies, Atmospheric Environment Service of Environment Canada, Downsview, Ontario, Canada

**Abstract.** Aerosol optical depth measurements acquired through the Canadian sunphotometer network were statistically analyzed for the **1987-1992** period in order to investigate spatial and temporal commonalities between the member stations. Four stations were chosen to yield a spatially representative sampling of atmospheric optical conditions across Canada (East Coast, eastern continental, western continental, and West Coast). All the stations were located in rural, local pollution free areas, The results of aerosol optical depth measurements showed significant differences between eastern and western Canadian stations. The effect of the Pinatubo volcanic eruption was clearly seen in the measurements acquired at Sable Island, Nova Scotia. Air mass relationships for the four stations sampled demonstrated the relevance of applying air **mass** classification criteria to the analysis and discrimination of atmospheric optical depth. Knowledge of the seasonal trend combined with information concerning air mass type enables a coarse a priori estimation of aerosol optical depth in the absence of traditional optical data. Synoptical air mass analysis facilitates the understanding of the mechanisms involved in the seasonal variations of aerosol optical depth and yields useful information about the atmospheric optical state. The relevance of the synoptical air mass approach was demonstrated in one particular case: a seasonal aerosol optical depth trend for Arctic air masses was observed for the three sunphotometer stations which regularily experience this type of air mass.

## 1. Introduction

Atmospheric monitoring in conditions of cloudless skies is a fundamental means of characterizing and understanding the mechanisms which contribute to aerosol variability. The prediction and quantitization of aerosol variability is an essential parameterization for numerous applications and a key parameter for monitoring this variability is the aerosol optical depth *[Penner et al.,* 1994].

Terrestrial remote sensing applications require information about aerosol optical variability inasmuch as aerosols are the unknown variable component which contribute to atmospheric backscatter (and hence the atmospheric masking effect) which must be corrected for in most terrestrial imaging applications.

Optical aerosol climatology [*d'Almeida et al.*, 19881 is a supplementary means for extracting information required in atmospheric correction methods. The validation of aerosol optical properties derived from satellite data requires further investigations of atmospheric aerosol optical state *[Kaufman and Tanré,* 1994]. Synoptic- to global-scale aerosol models are needed in order to evaluate the influence of anthropogenic aerosol on climate changes *[Penner et al.,* 19941.



Paper number 95JD02608.
0148-0227/96/95JD-02608$09.00

Since the measurement of aerosol optical depth on a global scale has always been a difficult problem, it **is** of considerable interest to examine the potential for characterizing the optical statistics of a base set of air mass types and accordingly to use the base set **as a** means for classifying the atmospheric optical state [*Smirnov et al.,* 1994; *Halthore et al.,* 19921.

**The** required optical statistics of the atmosphere ***are*** typically in the form of aerosol turbidity data acquired by solar photometry. Studies of atmospheric turbidity over Canada have been carried out by a number of research groups [*O'Neill et al.,* 1993; *Ahern et al.,* 1991; *Davies et al.,* 1988; *Hay and Darby,* 1984; *O'Neill and Miller,* 1984; *Freund,* 1983; *Uboegbulam and Davies,* 1983; *Polavarapu,* 19781. Although these studies employed similar sunphotometry techniques **as** those employed here, they did not incorporate a comprehensive investigation of the links between optical and synoptical information.

The goals of the present investigation are to consider the results of atmospheric optical depth measurements acquired through the Canadian sunphotometer network and to analyze the data set in order to estimate the dependence of mean and modal values of aerosol optical depth on air mass type. A number of representative stations are selected in order to adequately characterize the atmospheric optical properties across Canada. These are: Sable Island (East Coast, Nova Scotia), Sherbrooke (Quebec), Wynyard (Saskatchewan), Cape St. James (West Coast, British Columbia) (Figure 1). All the stations are situated in rural, pollution free areas.


**Figure 1.** Map of the four sunphotometer stations used in the study.

The Canadian sunphotometer network was part of the Background Air Pollution Monitoring Network (BAPMON). In a recent report [*Forgan et al.*, 19931 the uncertainities of the results obtained and the associated difficulties in their interpretation are pointed out clearly. Nonstablc instruments, poor calibration, the absence of the uniform processing procedure may significantly affect the data quality. Nevertheless, the report recommends the reanalysis of the turbidity archive in order to extract a suitable database for future studies of atmospheric turbidity trends.

## 2. Data Processing

Aerosol optical depths were derived from sunphotometer measurements performed at Sable Island, Nova Scotia (43°56' N, 60'01' W) in the period from October 1987 to August 1992; at Sherbrooke, Québec (45'24' N. 71'54' W), in the period from January 1989 to August 1991: at Wynyard, Saskatchewan (51'46' N, 104'12' W), in the period from March 1987 to April 1991 and at Cape St. James, British Columbia (51'46' N, 131°01' W), in the period from March 1987 to December 1989. Data at Sherbrooke was collected at fairly frequent intervals (less than half an hour), while measurements at the other stations were made 3 to 5 times daily.

The sunphotometer instruments employed two interference filters centered at 380 and 500 nm, according to the recommendations of the WMO. The same data processing procedure was applied to all the measurements. The notes written by the operators about sky conditions were also taken into account. Thus some values associated with clouds in the field of view were eliminated. The calibration constants of the instruments were checked using those data acquired on the clearest days. The original calibration constants and our postcalibration verifications indicated that the precision of the instruments was no worse than ±0.02 (see also *O'Neill et al.* [1993]). At the outset of this investigation we decided to avoid certain calibration problems which often affect the 380-nm ultraviolet channel and constrain ourselves to a study of optical depth measured at the more stable 500-nm channel.

In order not to overestimate the weight of those days for which many extinction measurements were made, we reduced the diurnal data sets to before noon and afternoon averages. The Sun position was estimated according to [*Michalsky*, 1988] and optical air masses were calculated using the formula derived by *Kasten* [1966]. Rayleigh optical depths were computed according to ***Russell et al.*** [1993]. The ozone optical depth was estimated by employing the latitudinal mean values of ***Robinson*** [1966] and absorption coefficients for ozone of ***Vigroux*** [1953] [e.g., *Iqbal*, 19831.

The data set for Sherbrooke was unique in that it was acquired with the same type of sunphotometer as the one described above but with four extra spectral channels. A detailed analysis of this data set and its relation to synoptical air mass for a single continental station was reported in a separate paper [*Smirnov et al.*, 19941. In the current paper we consider only the aerosol optical depth at 500 nm for all the stations of the network.

Thus in the text that follows, atmospheric optical state is characterized by one parameter: $\tau_a$ , which is the spectral aerosol optical depth at the wavelength 500 nm. The monthly mean values of aerosol optical depth ($\tau_a$), their standard deviations ($\sigma$), and the number of measurement series (N) can

**Table 1.** Database Summary for Sable Island, Nova Scotia

| | N | 1987 | N | 1988 | N | 1989 | N | 1990 | N | 1991 | N | 1992 |
|---|---|---|---|---|---|---|---|---|---|---|---|---|
| Jan. | ... | ... | 15 | 0.07 | 6 | 0.19 | 7 | 0.15 | ... | ... | ... | ... |
| | | ... | | 0.02 | | 0.06 | | 0.05 | | ... | | ... |
| Feb. | ... | ... | 9 | 0.15 | 7 | 0.15 | 5 | 0.10 | 2 | 0.15 | 4 | 0.27 |
| | | ... | | 0.06 | | 0.05 | | 0.03 | | 0.10 | | 0.05 |
| March | ... | ... | 9 | 0.10 | 14 | 0.13 | 15 | 0.14 | 9 | 0.16 | 8 | 0.33 |
| | | ... | | 0.02 | | 0.04 | | 0.05 | | 0.02 | | 0.08 |
| April | ... | ... | 8 | 0.14 | 10 | 0.15 | 17 | 0.17 | 17 | 0.18 | 14 | 0.32 |
| | | ... | | 0.05 | | 0.05 | | 0.03 | | 0.05 | | 0.14 |
| May | ... | ... | 13 | 0.20 | 9 | 0.19 | 9 | 0.15 | 23 | 0.15 | 16 | 0.39 |
| | | ... | | 0.11 | | 0.05 | | 0.04 | | 0.05 | | 0.06 |
| June | ... | ... | 10 | 0.13 | 6 | 0.17 | 10 | 0.25 | 7 | 0.18 | ... | ... |
| | | ... | | 0.06 | | 0.06 | | 0.09 | | 0.08 | | ... |
| July | ... | ... | 10 | 0.13 | 12 | 0.22 | 17 | 0.26 | 11 | 0.23 | 20 | 0.37 |
| | | ... | | 0.07 | | 0.05 | | 0.13 | | 0.03 | | 0.06 |
| Aug. | ... | ... | 11 | 0.13 | 25 | 0.27 | 23 | 0.22 | 8 | 0.37 | 11 | 0.35 |
| | | ... | | 0.05 | | 0.07 | | 0.08 | | 0.09 | | 0.07 |
| Sept. | ... | ... | 14 | 0.15 | 16 | 0.18 | ... | ... | 8 | 0.20 | ... | ... |
| | | ... | | 0.04 | | 0.05 | | ... | | 0.06 | | |
| Oct. | 21 | 0.13 | 14 | 0.16 | ... | ... | ... | ... | 13 | 0.24 | ... | ... |
| | | 0.05 | | 0.11 | | ... | | ... | | 0.06 | | |
| Nov. | 3 | 0.16 | 7 | 0.12 | 7 | 0.15 | ... | ... | 4 | 0.23 | ... | ... |
| | | 0.15 | | 0.04 | | 0.06 | | ... | | 0.05 | | |
| Dec. | 7 | 0.10 | 1 | 0.08 | 5 | 0.11 | ... | ... | 4 | 0.30 | ... | ... |
| | | 0.03 | | | | 0.05 | | ... | | 0.06 | | |
| Year | 31 | 0.12 | 120 | 0.13 | 117 | 0.19 | 102 | 0.19 | 106 | 0.21 | 73 | 0.35 |
| | | 0.06 | | 0.07 | | 0.07 | | 0.09 | | 0.08 | | 0.09 |
| Winter | ... | ... | 24 | 0.10 | 18 | 0.15 | 12 | 0.13 | 7 | 0.26 | 4 | 0.27 |
| | | ... | | 0.06 | | 0.06 | | 0.05 | | 0.08 | | 0.05 |
| Spring | ... | ... | 30 | 0.15 | 33 | 0.15 | 41 | 0.16 | 50 | 0.17 | 38 | 0.35 |
| | | ... | | 0.09 | | 0.05 | | 0.04 | | 0.05 | | 0.10 |
| Summer | ... | ... | 31 | 0.13 | 43 | 0.25 | 50 | 0.24 | 21 | 0.26 | 31 | 0.37 |
| | | ... | | 0.06 | | 0.07 | | 0.10 | | 0.10 | | 0.06 |
| Fall | 24 | 0.13 | 35 | 0.15 | 23 | 0.17 | ... | ... | 25 | 0.23 | ... | ... |
| | | 0.07 | | 0.08 | | 0.06 | | ... | | 0.06 | | ... |

The second row for each month is the standard deviation of $\tau_a$. N is the number of measurement series. Three centered dots indicate that no measurements are available.

be observed in Tables 1 to 4 (a "series" corresponds to a before noon or afternoon measurement set). These tables give a global viewpoint of the analyzed experimental data and the statistical characteristics during the measurement period. Gaps in the tables during the period of measurement are associated with the instrumental difficulties when no measurements were made.

## 3. Interannual Variability of Aerosol Optical Depth

Figure 2 shows the interannual and seasonal variability of aerosol optical depth for each station (each tick of the graph represents a single month) as a function of the total measurement period (top graphs) and as a function of season (bottom graphs). In Figures 3 and 4 we present aerosol optical depth histograms for the eastern (Sable Island and Sherbrooke) and western (Wynyard and Cape St. James) stations, respectively. The post-Pinatubo eruption data are shown separately (white columns for the fall 1991 and all 1992) on the Sable Island histogram (results for the fall of 1991 and in 1992 were available only for this station). It can be seen from Figures 2-4 and Tables 1-4 that the atmosphere in the eastern Canadian stations was typically more turbid (larger average values of $\tau_a$) and less stable (wider distributions or larger $\sigma$ values) than found in western Canada. In the summer of 1988 the aerosol optical depth across Canada was very low.

Monthly averages of $\tau_a$ for Sable Island are shown in Figure 2a. A "classical" annual pattern with a slow increase to maximal turbidity in the summertime [*Polavarapu*, 1978; *Malm and Walther*, 1979; *Peterson et al.*, 1981; *Uboegbulam and Davies*, 1983] is apparent in all the years besides 1988. A winter minimum is always in evidence except in 1992 (the effect of the Pinatubo eruption is discussed below).

The results for Sherbrooke are presented in Figures 2c and 2d. Maximal turbidity in the summertime is apparent only in 1989, while a winter minimum is always in evidence. Mean values for January to March as well as for September, November, and December stay nearly constant throughout the whole 3-year period of observation. Although the 3 months averaging incorporated in Figure 2d filters out much of the temporal variation, one can observe that the seasonal variability of aerosol optical depth in Sherbrooke is less than in Sable Island.

Mean monthly values of aerosol optical depth for Wynyard are shown in Figure 2e. One can observe certain differences between Wynyard and the other stations. In particular, the Wynyard results show a consistent maximum in the spring (cf. section 5.1 below). In general, the monthly averages of $\tau_a$ for

**Table 2.** Database Summary for Sherbrooke, Quebec

| | N | 1989 | N | 1990 | N | 1991 |
|---|---|---|---|---|---|---|
| Jan. | 7 | 0.10 | 6 | 0.14 | 17 | 0.10 |
| | | 0.02 | | 0.06 | | 0.03 |
| Feb. | 7 | 0.11 | 11 | 0.13 | 17 | 0.16 |
| | | 0.02 | | 0.04 | | 0.07 |
| March | 18 | 0.15 | 21 | 0.16 | 19 | 0.12 |
| | | 0.04 | | 0.07 | | 0.06 |
| April | 15 | 0.16 | 12 | 0.30 | 21 | 0.16 |
| | | 0.03 | | 0.15 | | 0.08 |
| May | 6 | 0.20 | 19 | 0.16 | 17 | 0.12 |
| | | 0.08 | | 0.06 | | 0.04 |
| June | 5 | 0.22 | 12 | 0.13 | 23 | 0.10 |
| | | 0.06 | | 0.02 | | 0.05 |
| July | ... | ... | 10 | 0.12 | 10 | 0.16 |
| | | ... | | 0.07 | | 0.07 |
| Aug. | 11 | 0.29 | 14 | 0.16 | 14 | 0.26 |
| | | 0.13 | | 0.06 | | 0.14 |
| Sept. | 10 | 0.14 | 9 | 0.14 | 3 | |
| | | 0.06 | | 0.08 | | |
| Oct. | 12 | 0.25 | 20 | 0.14 | ... | ... |
| | | 0.11 | | 0.10 | | ... |
| Nov. | 8 | 0.20 | 14 | 0.19 | ... | ... |
| | | 0.06 | | 0.15 | | ... |
| Dec. | 9 | 0.11 | 16 | 0.12 | ... | ... |
| | | 0.05 | | 0.05 | | ... |
| Year | 108 | 0.18 | 164 | 0.16 | 141 | 0.14 |
| | | 0.09 | | 0.09 | | 0.08 |
| Winter | 23 | 0.10 | 33 | 0.12 | 34 | 0.13 |
| | | 0.03 | | 0.05 | | 0.06 |
| Spring | 39 | 0.16 | 52 | 0.19 | 57 | 0.14 |
| | | 0.05 | | 0.10 | | 0.07 |
| Summer | 16 | 0.27 | 36 | 0.14 | 47 | 0.16 |
| | | 0.11 | | 0.05 | | 0.11 |
| Fall | 30 | 0.20 | 43 | 0.15 | ... | ... |
| | | 0.10 | | 0.11 | | ... |

Wynyard are lower than for Sable Island and Sherbrooke. The atmosphere here was remarkably pure, being characterized by mean monthly values which were usually less than 0.15. Figure 2f is unique with respect to the results observed for all other stations in that it indicates a fall-winter minimum at Wynyard instead of only the winter minimums observed for the other stations.

The relatively small number of measurements for Cape St. James made it difficult to formulate a clear description of the sampled West Coast optical properties. Nevertheless, one can observe in Figure 2 and Tables 1 to 4 that the West Coast atmosphere is more transparent than that represented by the East Coast data. A comparison of Figures 3 and 4 leads one to observe that Cape St.James is characterized by the narrowest probability distributions and, accordingly, the smallest standard deviations of $\tau_a$. Figure 2h, which presents the seasonal variability of aerosol optical depth, did not show any significant differences between the seasons.

Mean monthly values and standard deviations of aerosol optical depth for the total measurement period are shown in Figure 5. An annual cycle with maximum values in summer is evident only for Sable Island. A maximim of turbidity in spring and a minimum in the late fall (instead of the winter minimum characteristic of the other stations) can be observed for Wynyard. Because of the weak variability of optical properties at Cape St. James we would be hard put to consider the summer increase of $\tau_a$ as a significant annual cycle feature. Standard deviations for Sable Island and Sherbrooke generally increase with the mean values of $\tau_a$ ,but for Wynyard and Cape St. James, the $\sigma$ values do not vary significantly.

**Table 3.** Database Summary for Wynyard, Saskatchewan

| | N | 1987 | N | 1988 | N | 1989 | N | 1990 | N | 1991 |
|---|---|---|---|---|---|---|---|---|---|---|
| Jan. | ... | ... | 13 | 0.10 | 24 | 0.05 | 3 | 0.05 | 11 | 0.05 |
| | | ... | | 0.04 | | 0.02 | | 0.01 | | 0.02 |
| Feb. | ... | ... | 26 | 0.08 | 32 | 0.08 | 20 | 0.06 | 7 | 0.04 |
| | | ... | | 0.05 | | 0.04 | | 0.03 | | 0.02 |
| March | 7 | 0.11 | ... | ... | 29 | 0.10 | 15 | 0.08 | 15 | 0.12 |
| | | 0.04 | | ... | | 0.04 | | 0.03 | | 0.04 |
| April | 33 | 0.13 | 28 | 0.10 | 35 | 0.13 | 16 | 0.09 | 17 | 0.14 |
| | | 0.07 | | 0.04 | | 0.04 | | 0.02 | | 0.04 |
| May | 28 | 0.21 | 32 | 0.15 | 26 | 0.14 | 20 | 0.15 | ... | ... |
| | | 0.05 | | 0.05 | | 0.05 | | 0.04 | | ... |
| June | 26 | 0.16 | 28 | 0.12 | 23 | 0.10 | 17 | 0.11 | ... | ... |
| | | 0.06 | | 0.07 | | 0.03 | | 0.03 | | ... |
| July | 27 | 0.14 | 34 | 0.10 | 29 | 0.13 | 15 | 0.16 | ... | ... |
| | | 0.04 | | 0.04 | | 0.07 | | 0.05 | | ... |
| Aug. | 26 | 0.07 | 29 | 0.10 | 24 | 0.16 | 17 | 0.12 | ... | ... |
| | | 0.03 | | 0.05 | | 0.06 | | 0.03 | | ... |
| Sept. | 25 | 0.08 | 21 | 0.07 | 14 | 0.10 | ... | ... | ... | ... |
| | | 0.04 | | 0.03 | | 0.08 | | ... | | ... |
| Oct. | 22 | 0.08 | 26 | 0.06 | 14 | 0.05 | ... | ... | ... | ... |
| | | 0.05 | | 0.04 | | 0.01 | | ... | | ... |
| Nov. | 22 | 0.04 | 13 | 0.04 | 11 | 0.04 | ... | ... | ... | ... |
| | | 0.02 | | 0.02 | | 0.02 | | ... | | ... |
| Dec. | 12 | 0.06 | 20 | 0.06 | ... | ... | 6 | 0.06 | ... | ... |
| | | 0.03 | | 0.04 | | ... | | 0.03 | | ... |
| Year | 228 | 0.11 | 270 | 0.09 | 261 | 0.11 | 129 | 0.11 | 50 | 0.10 |
| | | 0.07 | | 0.05 | | 0.06 | | 0.05 | | 0.05 |
| Winter | 12 | 0.06 | 59 | 0.08 | 56 | 0.06 | 29 | 0.06 | 18 | 0.05 |
| | | 0.03 | | 0.05 | | 0.04 | | 0.02 | | 0.02 |
| Spring | 60 | 0.15 | 60 | 0.12 | 90 | 0.12 | 51 | 0.11 | 32 | 0.13 |
| | | 0.07 | | 0.05 | | 0.05 | | 0.04 | | 0.04 |
| Summer | 79 | 0.12 | 91 | 0.10 | 76 | 0.13 | 49 | 0.13 | ... | ... |
| | | 0.06 | | 0.05 | | 0.06 | | 0.04 | | ... |
| Fall | 69 | 0.07 | 60 | 0.06 | 39 | 0.07 | ... | ... | ... | ... |
| | | 0.04 | | 0.03 | | 0.06 | | ... | | |

**Table 4.** Database Summary for Cape St. James, British Columbia

| | N | 1987 | N | 1988 | N | 1989 |
|---|---|---|---|---|---|---|
| Jan. | ... | ... | ... | ... | ... | ... |
| | | ... | | ... | | ... |
| Feb. | ... | ... | 4 | 0.09 | 8 | 0.06 |
| | | ... | | 0.03 | | 0.01 |
| March | 0 | 0.09 | 9 | 0.07 | 13 | 0.07 |
| | | 0.02 | | 0.02 | | 0.02 |
| April | 8 | 0.12 | 19 | 0.10 | 24 | 0.10 |
| | | 0.05 | | 0.04 | | 0.03 |
| May | ... | ... | 5 | 0.12 | 11 | 0.12 |
| | | ... | | 0.03 | | 0.04 |
| June | 15 | 0.14 | 12 | 0.09 | ... | ... |
| | | 0.05 | | 0.04 | | ... |
| July | 11 | 0.09 | 13 | 0.09 | ... | ... |
| | | 0.03 | | 0.04 | | ... |
| Aug. | 14 | 0.09 | 7 | 0.09 | ... | ... |
| | | 0.04 | | 0.03 | | ... |
| Sept. | 3 | 0.08 | 7 | 0.07 | 2 | 0.08 |
| | | 0.01 | | 0.03 | | 0.04 |
| Oct. | 11 | 0.10 | 8 | 0.08 | 8 | 0.12 |
| | | 0.04 | | 0.04 | | 0.08 |
| Nov. | 4 | 0.06 | 2 | 0.06 | 8 | 0.08 |
| | | 0.02 | | 0.01 | | 0.04 |
| Dec. | 2 | 0.04 | 7 | 0.07 | 3 | 0.05 |
| | | 0.00 | | 0.03 | | 0.02 |
| Year | 78 | 0.10 | 93 | 0.09 | 77 | 0.09 |
| | | 0.05 | | 0.04 | | 0.05 |
| Winter | ... | ... | 11 | 0.08 | 11 | 0.06 |
| | | ... | | 0.03 | | 0.01 |
| Spring | 18 | 0.11 | 33 | 0.10 | 48 | 0.10 |
| | | 0.04 | | 0.04 | | 0.04 |
| Summer | 40 | 0.11 | 32 | 0.09 | ... | ... |
| | | 0.05 | | 0.04 | | ... |
| Fall | 18 | 0.09 | 17 | 0.07 | 18 | 0.10 |
| | | 0.04 | | 0.03 | | 0.06 |

### 3.1. Aerosol Optical Depth After the Pinatubo Eruption

Only the measurements obtained from Sable Island (43°56' N) were usable in the study of the aerosol optical depth increase induced by the Pinatubo eruption in June 1991. According to the data of *Valero and Pilewskie* [1992] the latitudinal distribution of extinction shows that by the middle of July the volcanic cloud had extended to 30° N.

On Figure 2a one can observe, beginning in October 1991, a consistent increase in $\tau_a$. Instead of a winter minimum which was typical for this station, the aerosol optical depth in the winter of 1991-1992 was twice the value expected from historical data. In Figure 3 we can observe how the histogram contribution associated with post-Pinatubo measurements (white columns in Figure 3) influenced the changes of the distribution in all the seasons. We would like to point out that according to our data for Sherbrooke and Sable Island, high optical depth values in the late summer of 1991 were probably not influenced by the Pinatubo cloud: the synoptic air mass analysis discussed below did not show any anomalies in August 1991.

According to *Dutton et al.* [1994] the stratospheric optical depth at 500-nm wavelength, 12 to 14 months after the Pinatubo eruption, was 0.10. For our data set it means that instead of typical summer values of 0.16-0.30 (see Figure 3c), optical depths measured at Sable Island were as high as 0.26-0.40.

Our results for the late fall of 1991 and 1992 correspond well with optical depth data obtained at Tucson, Arizona after the Pinatubo eruption (J.Simpson, personal communication, 1993). The similarity of the results at Mauna Loa [*Dutton et al.*, 1994], at Tucson, and at Sable Island is notable, especially because the latter data were acquired by a sunphotometer network during routine measurements.

## 4. Air Mass Analysis and Geographical Source Identification

The principles of air mass analysis, outlined by *Smirnov et al.* [1994] for Sherbrooke, were applied to the other three stations. A single surface weather chart, synchronized as closely as possible to measurement times, was used as a snapshot of the air mass distribution over North America. The analysis was performed by a human analyst and is similar to what can be done in the operational manner using ordinary weather data alone. We follow a traditional air mass classification that assumes the existence of two main fronts, polar and Arctic, and thus three air mass types, Arctic, polar, and tropical, with maritime and continental versions.

The four stations arc spread over a 6000-km belt and separated by mountains, plains and coastal zones. They are affected by different circulation mechanisms and are influenced in different proportions by Arctic, polar, and tropical air masses (Figure 6; see also Table 5 for air mass codes). While using a somewhat generalized common air mass classification suitable for all four stations, we try to preserve a site specific approach that allows us to perform even more detailed analysis. The subdivision of Pacific air in three subgroups for Wynyard and that of continental polar air for Sherbrooke are examples of this approach.

Surface weather maps (0000, 0600, 1200, and 1800 UT) for North America on microfilms provided by the Canada Climate Centre were used in this analysis. These maps are similar to the NOAA maps used for Sherbrooke [*Smirnov et al.*, 1994] in terms of information content but cover a larger territory. This feature enabled the analysis of wide sectors of the Atlantic and Pacific Oceans and thus permited reliable air mass analysis for the coastal stations at St. James and Sable Island. These maps, which also cover the Canadian North and the adjacent sector of the Arctic Ocean, ensure that the analysis of Arctic air masses was made as reliable as possible within the limits of available weather data. Twelve hourly (0000 and 1200 UT) maps for the 850, 700, 500, and 250-mbar levels were also available to us in the same data set. More detailed analysis involving these higher level maps and back trajectory tracing procedure was performed to resolve the more difficult cases. Surface conditions were given preference if a substantial difference was observed between the circulation pattern at the surface and that at higher levels.

The Sable Island station is situated on a small island, 300 km west of the Nova Scotia coast. Being all the time in the vicinity of a major frontal zone that follows the East Coast, it is influenced by all air masses present in our classification (except the Pacific air) and is thus a perfect observation site for our purposes. True maritime air, either Arctic, polar, or tropical, is often present at Sable Island. On the other hand, it is still under the influence of virtually unchanged continental air masses (Arctic and polar) for more than 50% of the observation period (Figure 6).

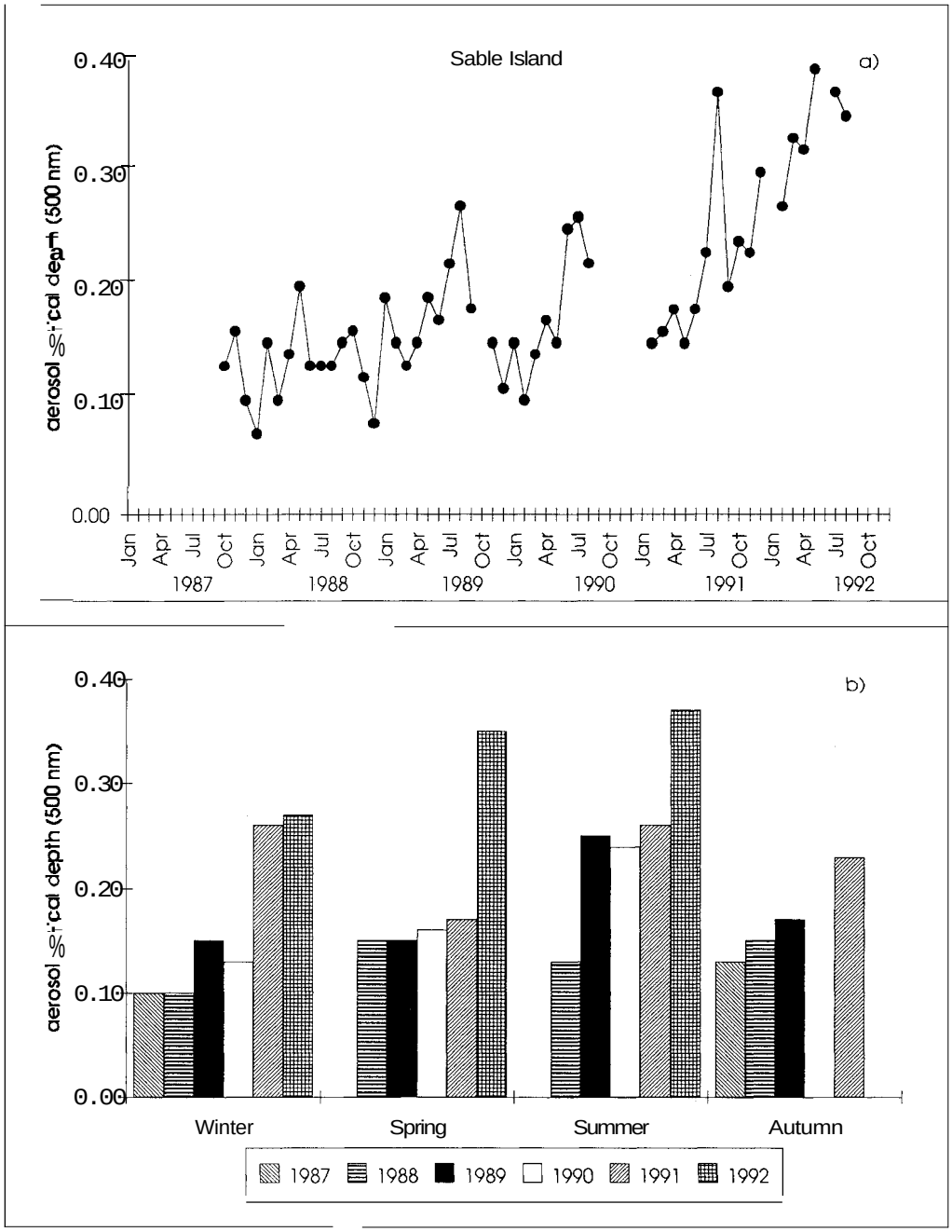


**Figure 2.** Mean monthly and seasonal values of aerosol optical depth at 500-nm wavelength for (a, b) Sable Island; (c, d) Sherbrooke; (e, f) Wynyard; and (g, h) Cape St. James. Winter corresponds to December, January, and February; spring corresponds to March, April, and May; summer corresponds to June, July, and August; fall corresponds to September, October and November.

Maritime Arctic air reaches Sable Island from the Labrador Sea via Newfoundland and the Labrador peninsula. Maritime polar air advances from the southwest in slow-moving high-pressure systems or from the North Atlantic, reaching this site with easterly flow in the rear parts of cyclones. Continental Arctic, polar, and occasionally tropical air arrives from a funnel-shaped sector between Hudson Bay in the north and the Great Lakes in the south. The last circulation pattern **is** most common here.

Maritime tropical air moves along the East Coast and reaches Sable Island more often than any other station included in our analysis. In some cases it arrives directly from the south and provides a pure sample of maritime air but more often it follows the U.S. coast and therefore can be somewhat contaminated.

The circulation pattern at Sherbrooke **is** analyzed in depth by ***Smirnov et al.*** [1994]. It is worth mentioning here that the Sherbrooke region is right at the center of an area that is not dominated by any single air mass type and characterized by *Bryson* [1966] as "indeterminate mixtures" of all types. Indeed, all air mass types mentioned before are present here in any season of the year, with a relatively frequent occurrence of

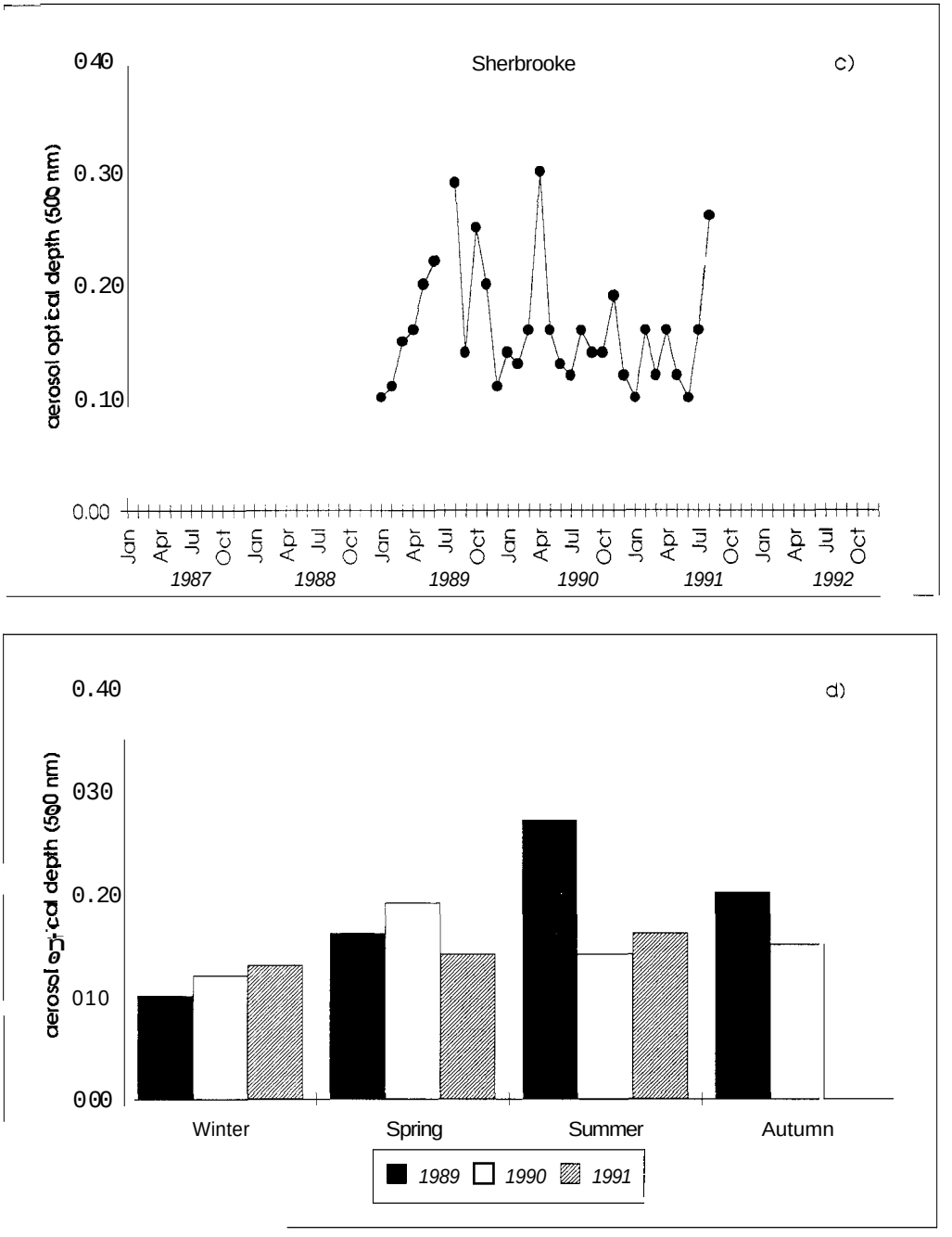


**Figure 2.** (continued)

tropical air. Maritime air from the Atlantic, either Arctic or polar, also reaches this area. We note, however, that although Sherbrooke is only 300 km from the East Coast, Atlantic air is rare and cannot truly be called maritime even when it does occur. This area is still affected by the strong westerly flow across North America that brings maritime air from the Pacific coast across the Cordillera. It is originally polar maritime air from the Pacific that flows slowly through Cordillera valleys and undergoes different degrees of modification, depending on trajectory and speed. Although often called Pacific air by climatologists, there is no agreement on its designation as maritime or continental [*Bryson*, 1966]. Pacific air still accounts for more than **30%** of air masses in the area but **is** completely modified by the time it reaches Sherbrooke and is considered polar continental in our analysis. This air is subdivided in three subgroups, north, west and south, according to its back trajectory over North America.

Wynyard, Saskatchewan, represents the large central North American plains far removed from the surrounding oceanic basins. The nearest large water body is Hudson Bay some, 1000 km northeast of Wynyard. The topography is flat, except for the eastern fringe of the Rocky Mountains, 800 km to the west. Although the adjacent surface is homogeneous, we should keep in mind that the immediate vicinity and the whole southern sector are agricultural land, whereas land to the north of Wynyard is mostly forested. This difference is likely to influence the respective atmospheric aerosol properties.

During the winter the Wynyard station is exposed to

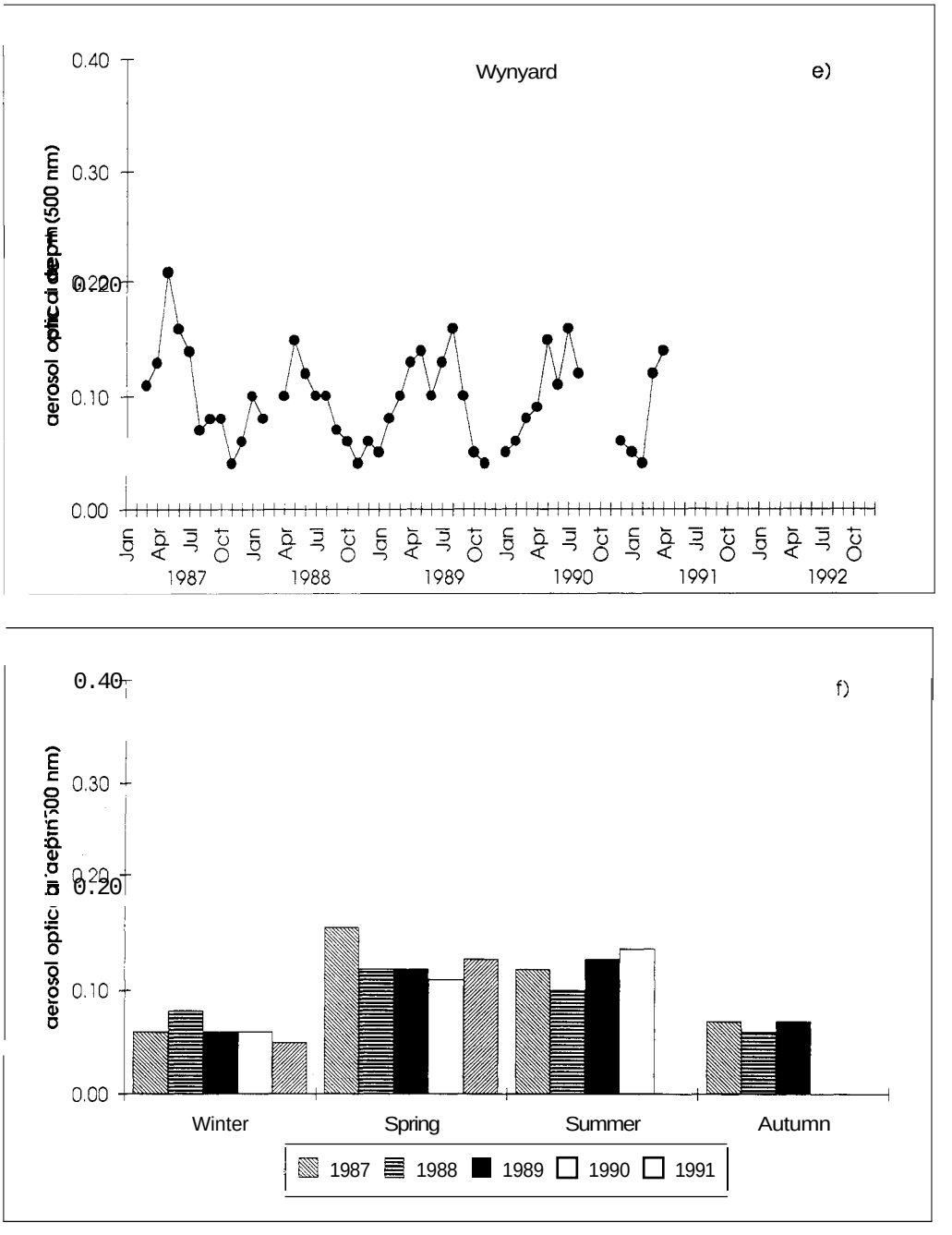


**Figure 2.** (continued)

topographically guided continental Arctic advections from the Canadian northwest. In summer this circulation pattern is less frequent and the air is classified as continental polar rather than Arctic; a secondary source of this air is clearly seen on July climatic maps in the high pressure zone centered over Hudson Bay [*Bryson*, 19661. Maritime arctic as well as Atlantic air does not reach this area. Most of the continental polar air observed at Wynyard is from the north and northeast and corresponds to the northern continental polar (cPn) subgroup at Sherbrooke. When Wynyard is dominated by a high-pressure zone with weak gradients, the residence time of a Pacific air mass over the continental plains can be as long as a week or two. This local air at Wynyard is also considered to be polar continental.

Air reaching Wynyard from the west and southwest is mostly of Pacific origin. Advections of Pacific air are not associated with pronounced atmospheric fronts. Since it is difficult to identify an air parcel crossing several major mountain ridges, most occurrences are simply designated "Pacific air." Two particular subgroups were defined within this type, the first being the air crossing the Cordillera much farther to the south in the United States (Wyoming to Montana) and moving north afterward (Pacific southwest). The second is Pacific air associated with pronounced chinook (foehn) events in Alberta

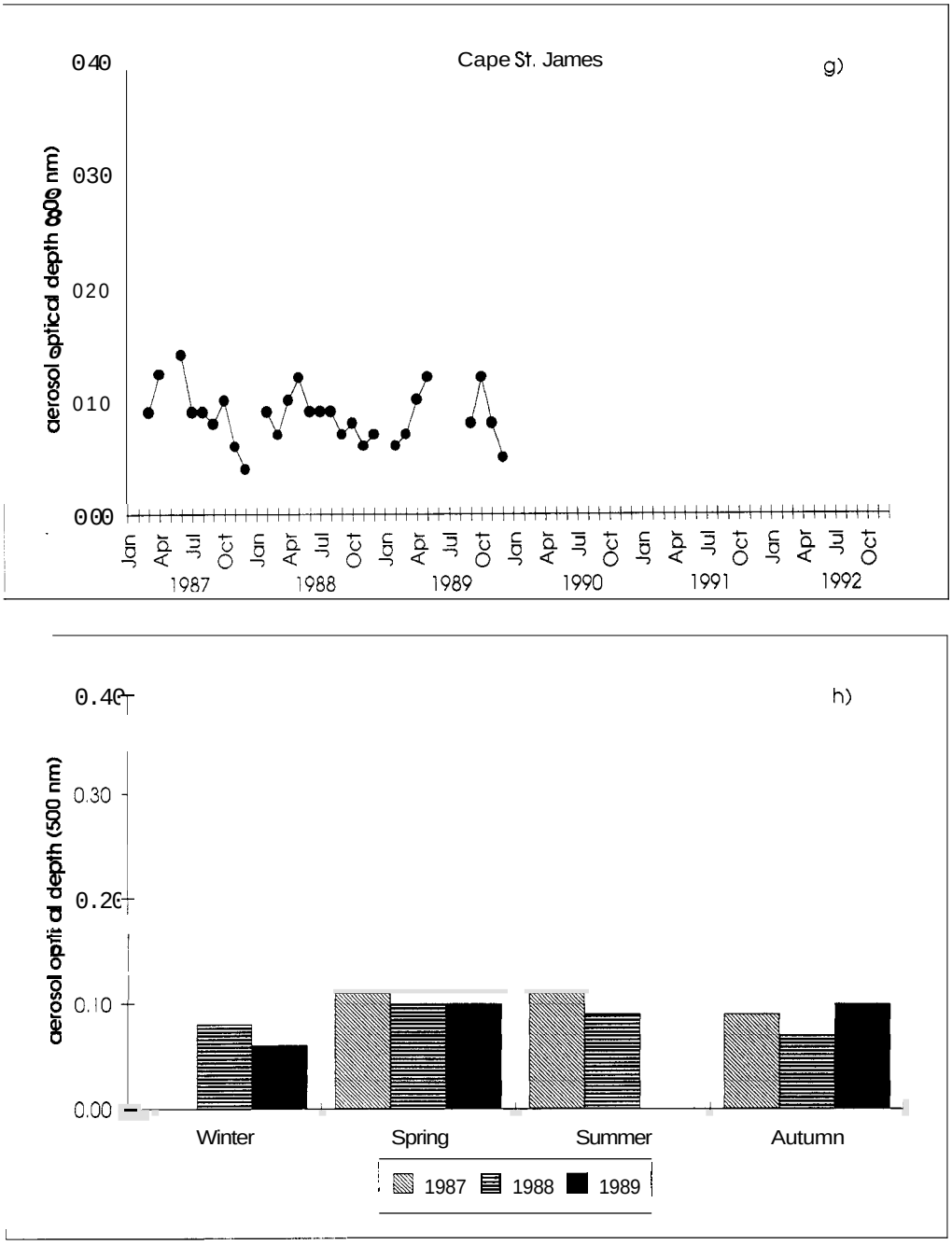


**Figure 2.** (continued)

(Pacific chinook). The latter is easily identified, especially in winter, by a strong westerly flow between the surface and 500 mb over the Cordillera as well as by a zone of unusually warm air 300-400 km wide east of the mountains. We assume that in these cases, air crosses the mountains in a different way than it normally does and can therefore have particular optical properties.

Tropical air is uncommon in the area and, even in July, accounts for less than 5% of occurrences [*Bryson,* 19961. This low-probability condition results because the dominant westerly flow intercepts and redirects northbound tropical masses to the Great Lakes and farther east. We have nevertheless recorded these rare events since aerosol properties of tropical air masses are likely to be very different from other air mass states. It can be concluded that Wynyard is dominated by northern continental air masses (Arctic and polar) and Pacific air.

The Cape St. James station, British Columbia, is situated at the southern tip of Queen Charlotte Island, some **200** km off the West Coast. It is exposed almost exclusively to the westerly flow of maritime polar air from the Pacific. Arctic advections are intercepted by the Alaskan mountains, while tropical air never reaches this latitude along the West Coast because of the dominant counter air mass flow associated with the cold southbound Californian current. The 1000-km-wide Cordillera in the East makes continental air advections toward

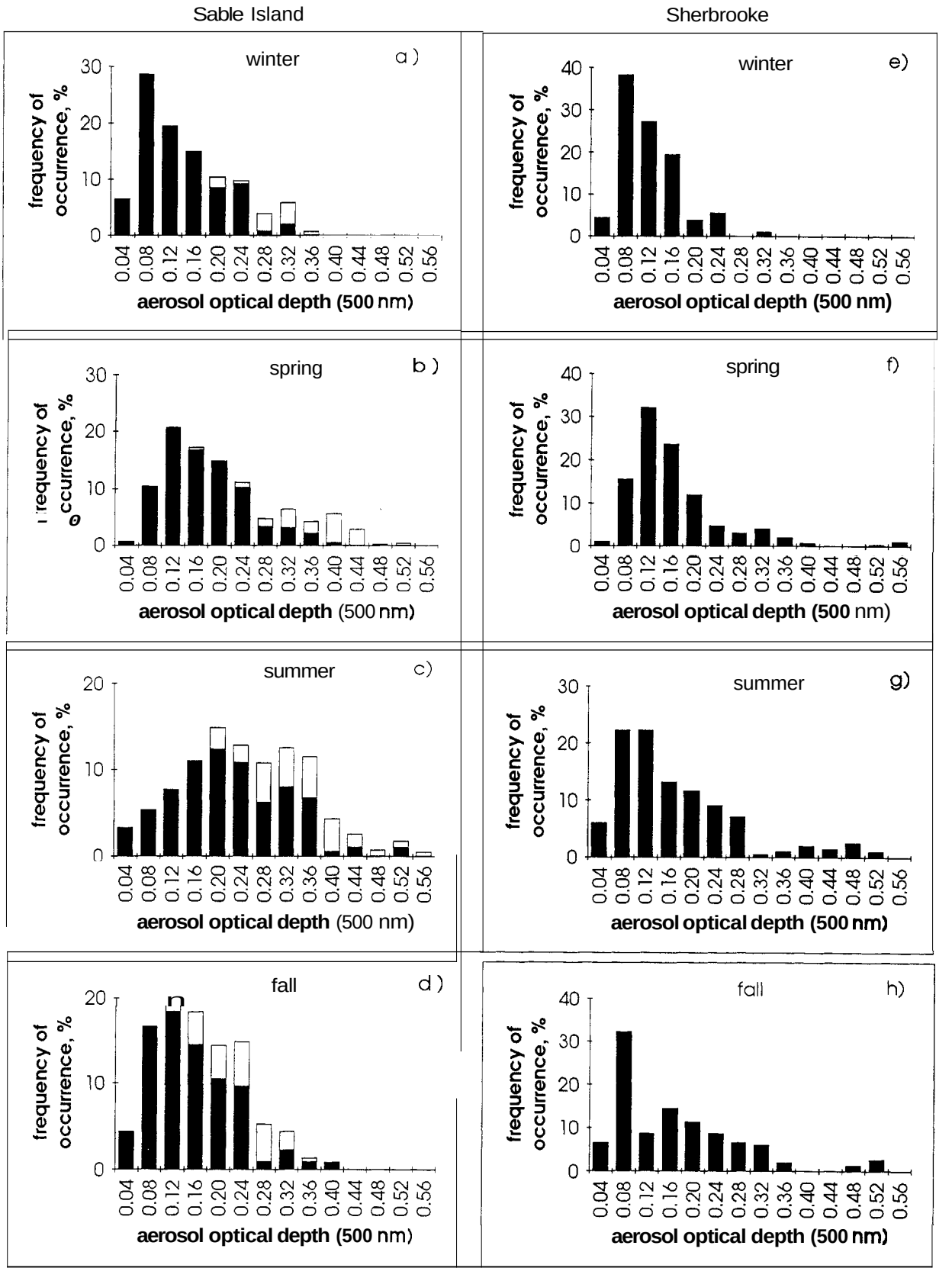


**Figure 3.** Seasonal frequency of occurrence of aerosol optical depth for Sable Island **(a-d)** and Sherbrooke (e-h). The sum of all frequences is equal to 100% for each season. Black columns correspond to pre-Pinatubo data; white columns correspond to post-Pinatubo data.

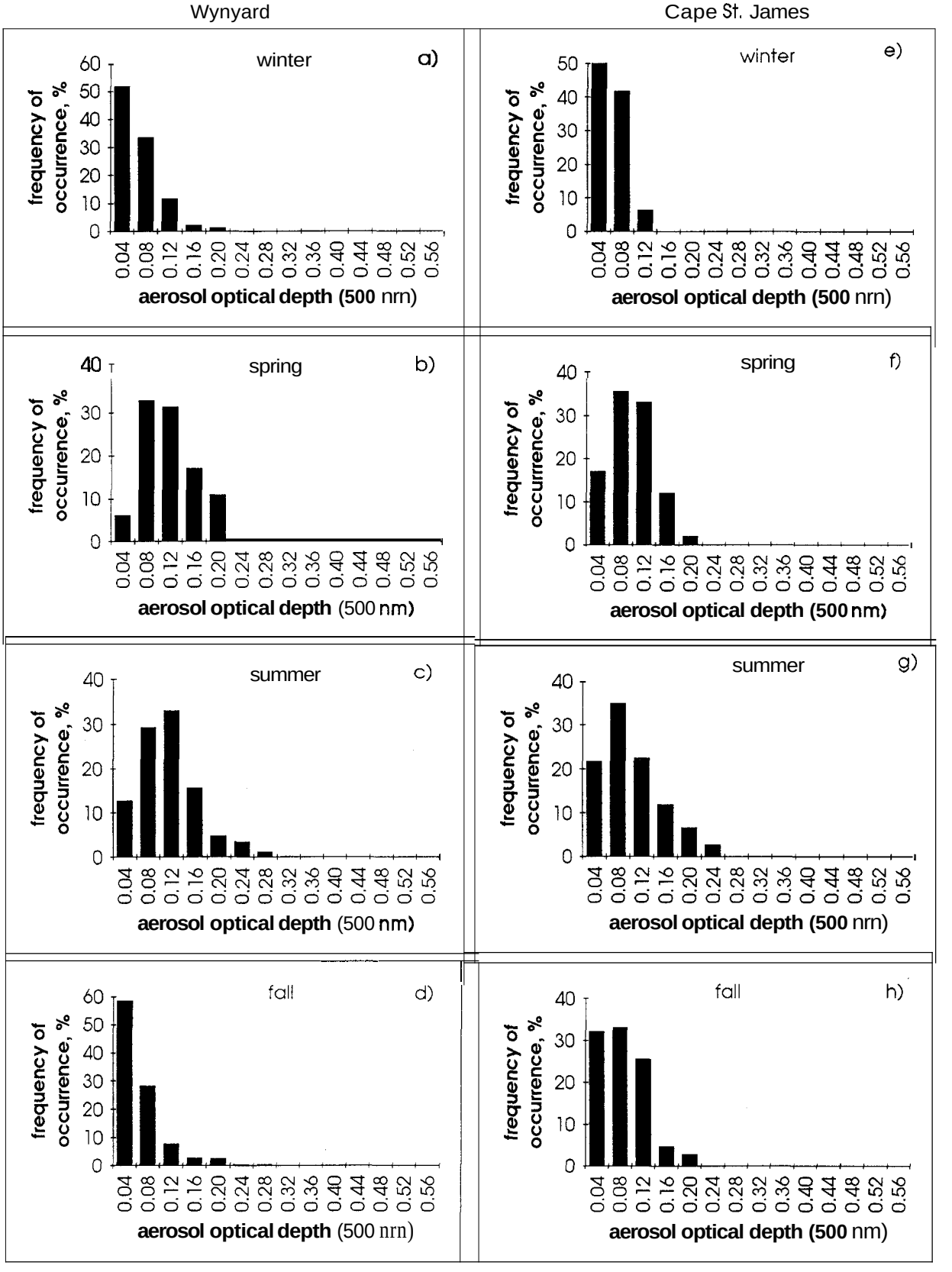


**Figure 4.** Seasonal frequency of occurrence of aerosol optical depth for (a-d) Wynyard and (e-h) Cape St. James. The sum of all frequences is equal to 100% for each season.

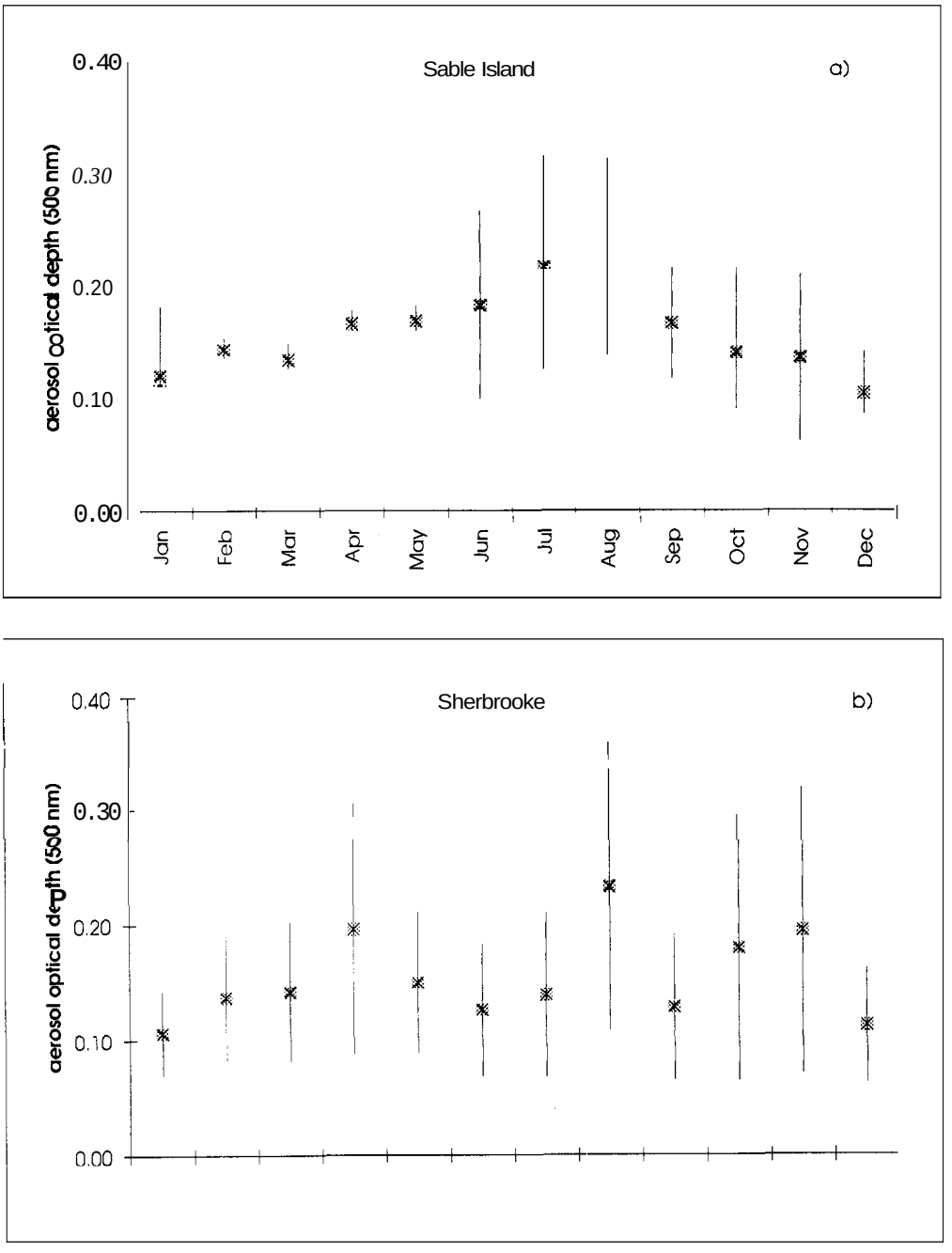


**Figure 5.** Mean monthly values of aerosol optical depth at the wavelength 500 nm for the whole period of measurements for (a) Sable Island, (b) Sherbrooke, (c) Wynyard, and (d) Cape St. James. The bars indicate plus or minus one standard deviation.

the coast impossible; the only possible, though negligeable. source of continental aerosol is thus the narrow coastal zone where the circulation pattern sometimes favors air movement along the coast either from the south or from the north. Cape St. James is thus dominated by the same maritime polar air mass type all year-round.

It is noted that Figure 6 shows the contribution of various air masses on the days of measurements, i.e., the cloudless days and days with few clouds (see Table 5 for air mass codes). The contribution of each air mass type changes substantially from station to station. As some weather maps were not available for analysis, the final statistics (total number of series considered) in Table 5 may be slightly different from Tables 1 to 4.

## 5. Optical Properties of Various Air Masses

To analyze the peculiarities of the interannual and seasonal variability of $\tau_a$, we considered temporal trends in air mass occurrence and mean monthly values of $\tau_a$ for the whole period of measurements (Figures 7a, 7b, 7c and 7d). These figures illustrate well the influence of air mass types on the seasonal

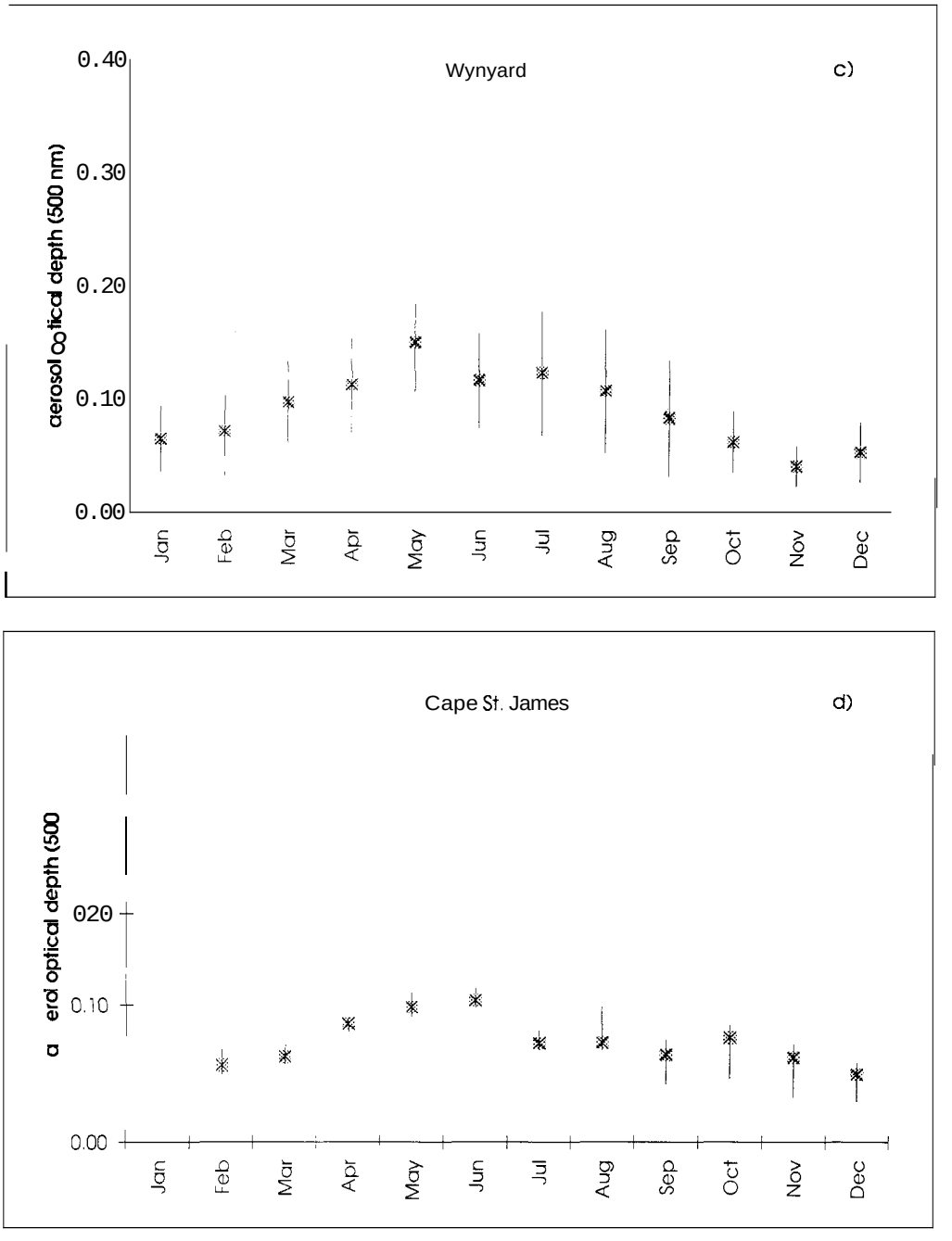


**Figure 5.** (continued)

variation of atmospheric optical parameters (cf. Table 5 for the relation between average aerosol optical depth and air mass type).

For Sable Island (Figure 7a) the influence of Arctic and tropical air on $\tau_a$ is well demonstrated by the interannual variability of aerosol optical depth. Mean monthly values significantly increase in summer when the Arctic air frequencies decrease and the tropical frequencies increase. The values decrease in the other months with the preponderance of less turbid polar air and, in particular, decrease to their lowest value when Arctic air is dominant.

An interesting example of the influence of tropical air (and the pertinence of the air mass technique) is the apparent but small increase in $\tau_a$ seen in February and in November. These increases correspond to a relatively larger proportion of tropic air masses (high $\tau_a$ ) for these months. In the months before and after these apparent increases the greater contributions of Arctic air masses induced more transparent conditions. A total absence of Arctic air during the January measurements of 1989 caused higher turbidity compared to 1988 and 1990. In the summer of 1988 the maritime Arctic and maritime polar air were responsible for low $\tau_a$ values (Figure 2).

The interannual summer minimum at Sherbrooke is associated with the dominance of Arctic air in June, while the distinct increase in turbidity in August and the fall period is an artifact of the tropical air contribution. The above mentioned

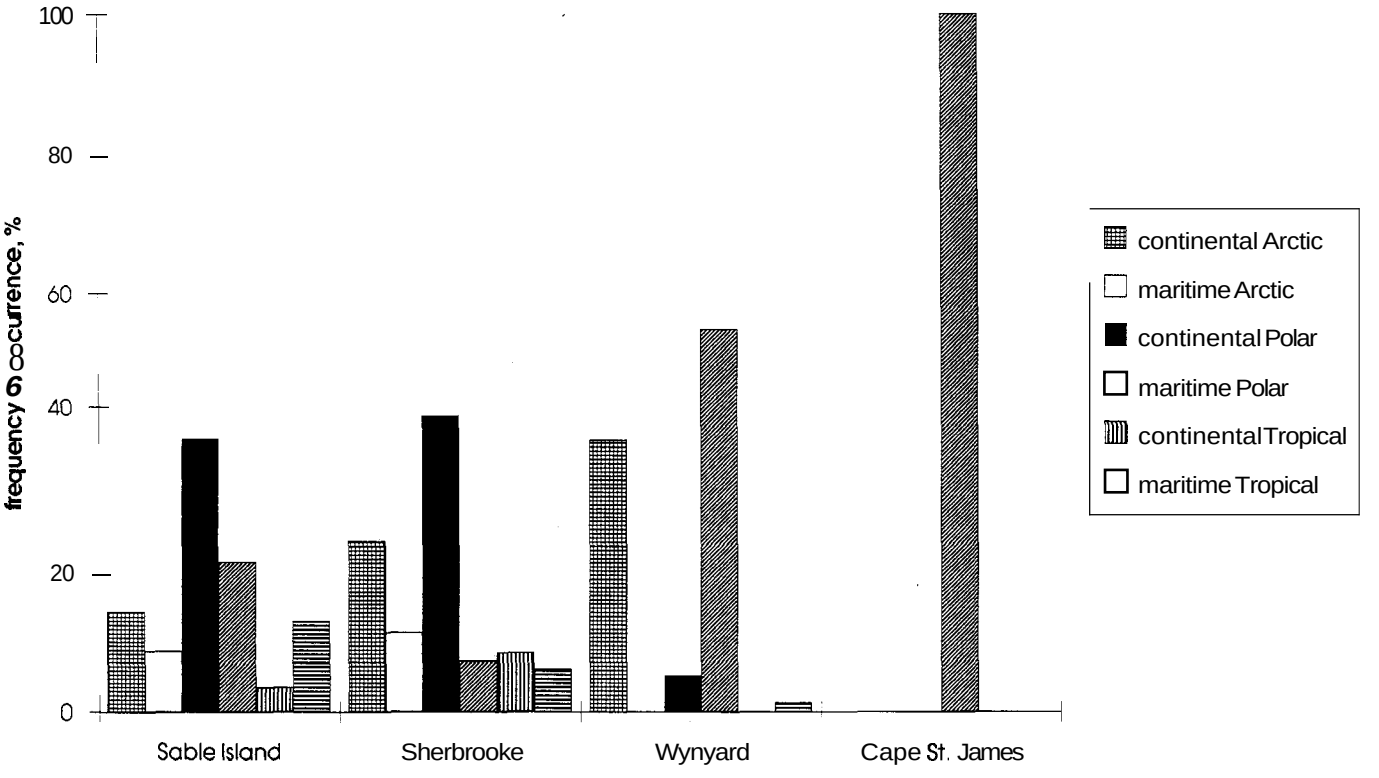


**Figure 6.** Frequency of occurrence of various air masses for all measurement days at each station. The sum of all frequences is equal to 100% for each station. See Table 5 for the air mass codes.

**Table 5.** Mean Optical Characteristics of Different Air Mass Classes

| | | Sable Island | | | Sherbrooke | | | Wynyard | | | Cape St. James | | |
|---|---|---|---|---|---|---|---|---|---|---|---|---|---|
| | Code | N | $\tau_a$ | σ | N | $\tau_a$ | σ | N | $\tau_a$ | σ | N | $\tau_a$ | σ |
| Arctic | | 100 | 0.12 | 0.04 | 148 | 0.10 | 0.03 | 327 | 0.08 | 0.04 | ..... | | ... |
| Continental Arctic | cA | 62 | 0.11 | 0.04 | 101 | 0.10 | 0.03 | 327 | 0.08 | 0.04 | ..... | | ... |
| Maritime Arctic | mA | 38 | 0.13 | 0.05 | 47 | 0.10 | 0.03 | ... | ... | ... | ..... | | ... |
| Polar | | 262 | 0.16 | 0.06 | 205 | 0.15 | 0.05 | 504 | 0.10 | 0.05 | 229 | 0.09 | 0.04 |
| Continental polar | cP | 169 | 0.17 | 0.06 | 175 | 0.15 | 0.05 | 43 | 0.12 | 0.05 | ..... | | ... |
| Maritime polar | mP | 93 | 0.15 | 0.06 | 30 | 0.17 | 0.06 | 461 | 0.10 | 0.05 | 229 | 0.09 | 0.04 |
| Tropical | | 71 | 0.26 | 0.09 | 60 | 0.32 | 0.10 | 11 | 0.22 | 0.06 | ..... | | ... |
| Continental tropical | cT | 15 | 0.25 | 0.06 | 35 | 0.32 | 0.11 | ... | ... | ... | ..... | | ... |
| Maritime tropical | mT | 56 | 0.27 | 0.10 | 25 | 0.31 | 0.09 | 11 | 0.22 | 0.06 | ..... | | ... |
| Continental polar | | | | | | | | | | | | | |
| North | cPn | | | | 58 | 0.12 | 0.03 | | | | | | |
| West | cPw | | | | 75 | 0.16 | 0.05 | | | | | | |
| south | cPs | | | | 42 | 0.18 | 0.04 | | | | | | |
| Maritime polar | | | | | | | | | | | | | |
| Pacific | | | | | | | | 335 | 0.11 | 0.05 | | | |
| Pacific (chinook) | | | | | | | | 80 | 0.06 | 0.03 | | | |
| Pacific southwest | | | | | | | | 46 | 0.15 | 0.05 | | | |

N is the number of analyzed series; $\tau_a$ is the aerosol optical depth at 500 nm; σ is the standard deviation of the aerosol optical depth. Three centered dots indicates that no measurements are available.

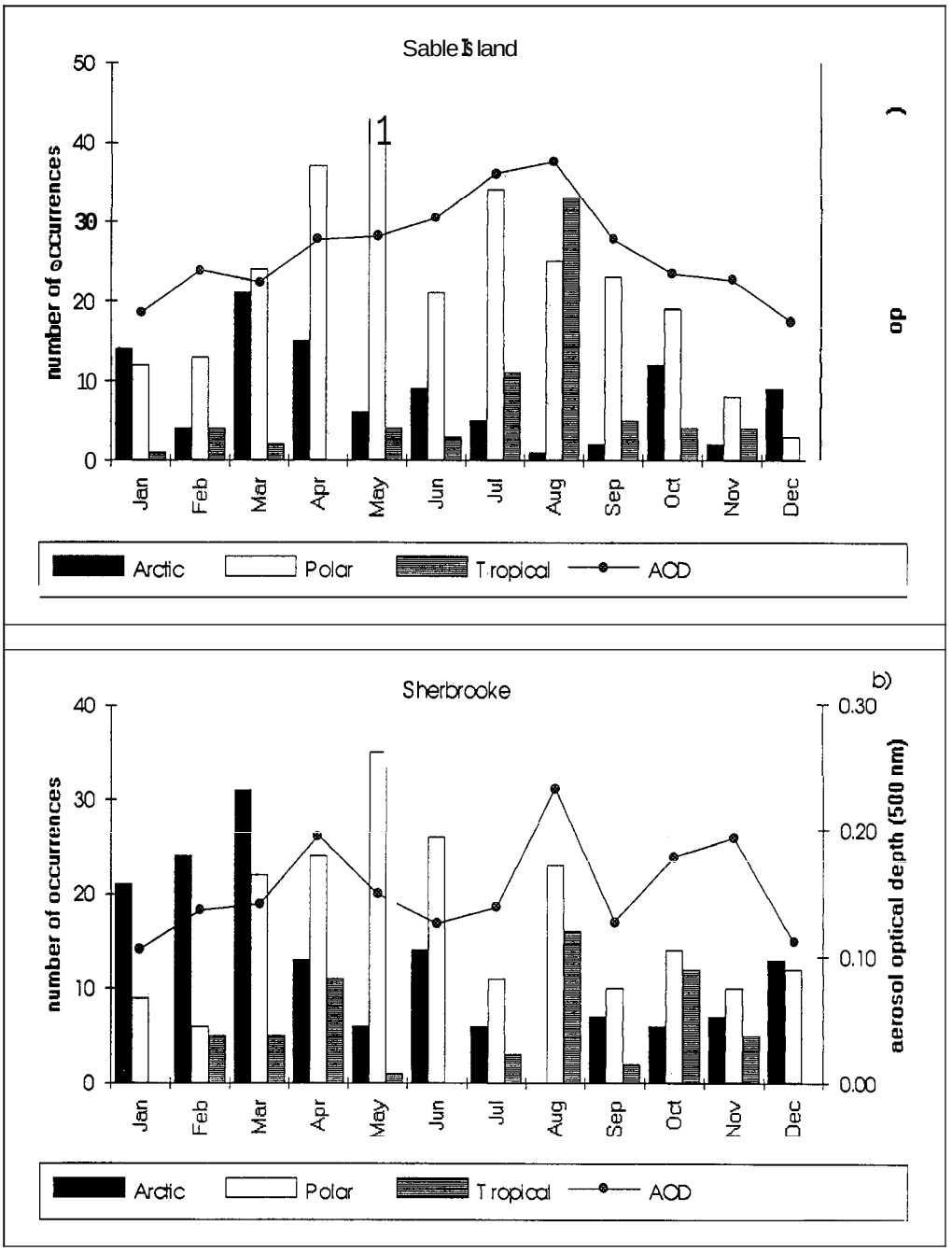


**Figure 7.** Mean monthly values of aerosol optical depth (circles and right-hand axis) and corresponding number of occurrences of various air masses (left-hand axis) for (a) Sable Island, (b) Sherbrooke, (c) Wynyard, and (d) Cape St. James.

summer minimum of $\tau_a$ in 1990 occurred owing to the unusually numerous intrusions of Arctic air between April and November, when polar and tropical air masses are normally more common. A more detailed analysis of the interannual and seasonal variability of aerosol optical depth over Sherbrooke during each measurement year can be found in the work of *Smirnov et al.* [1994].

For all practical purposes there was no real tropical air at Wynyard during the measurement period (Figures 6 and 7). Accordingly, the interannual variations of $\tau_a$ ought to follow the changes in the relationship between the number of Arctic and polar air mass occurrences. However, the composition of polar air at Wynyard is unusually quite complex, as will be seen in Figures 8 and 9 (see also section **4).**

The seasonal variations of the number of air mass occurrence at Cape St. James can be observed in Figure 7d. Our mean monthly values are in good agreement with the long-term measurements at Vancouver reported by *Hay and Darby* [1984]. Their nonspectral aerosol optical depth values were converted to $\tau_a(500)$ with a regression relationship developed especially for the kind of instruments employed in the current study [*Uboegbulam and Davies*, 19831. The difference between mean

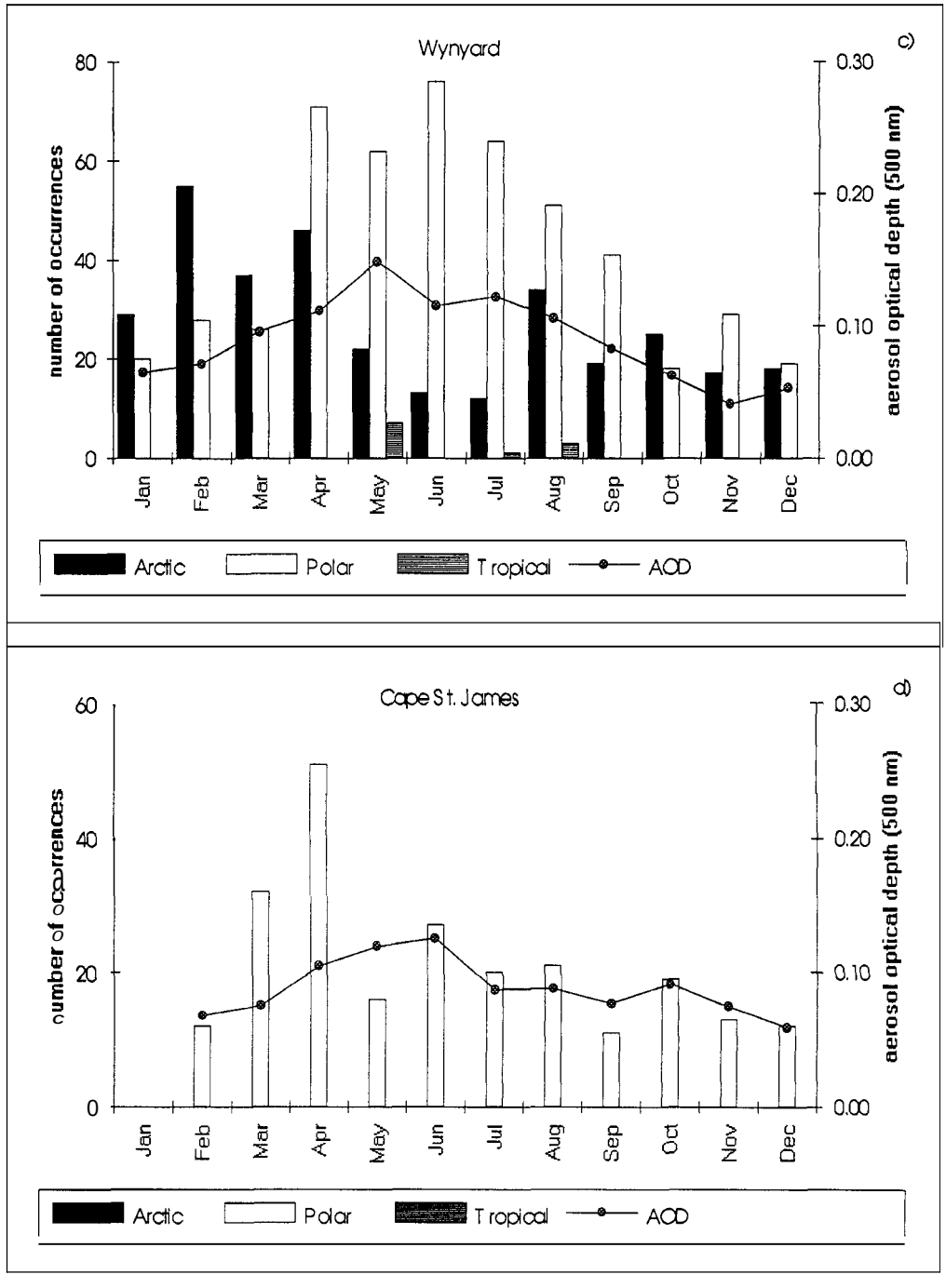


**Figure 7.** (continued)

monthly values did not exceed 0.02 for all the months except July and August.

A preliminary analysis based on the initial classification of Arctic, polar and tropical air masses yielded the results shown in Figure 8 (the sum of all frequencies **is** equal to 100% for each air mass type) and the relevant statistics can be found in Table **5.** For each station the differences between mean values of $\tau_a$ for Arctic, polar, and tropical air are statistically significant at the 95% level.

The frequency distributions for Sable Island and Sherbrooke are in good agreement (Figures 8a and 8b). It is notable that the distribution for Arctic air is wider at Sable Island than at Sherbrooke and, conversely, that at Sherbrooke the tropical air mass distribution is broader. This variability is likely associated with the different history of air prior to its arrival and the dissimilar aerosol contributions from local sources. For example, continental Arctic air arriving at Sable Island has a higher probability of contamination than polar maritime air from the North Atlantic. This is also true for tropical air as it travels to Sherbrooke. The same reasoning can be used to explain the difference in mean $\tau_a$ values for these two stations (see Table **5).**

Table **5** which includes polar air mass subclassification results for Sherbrooke [*Smirnov et al.*, 1994] demonstrates the

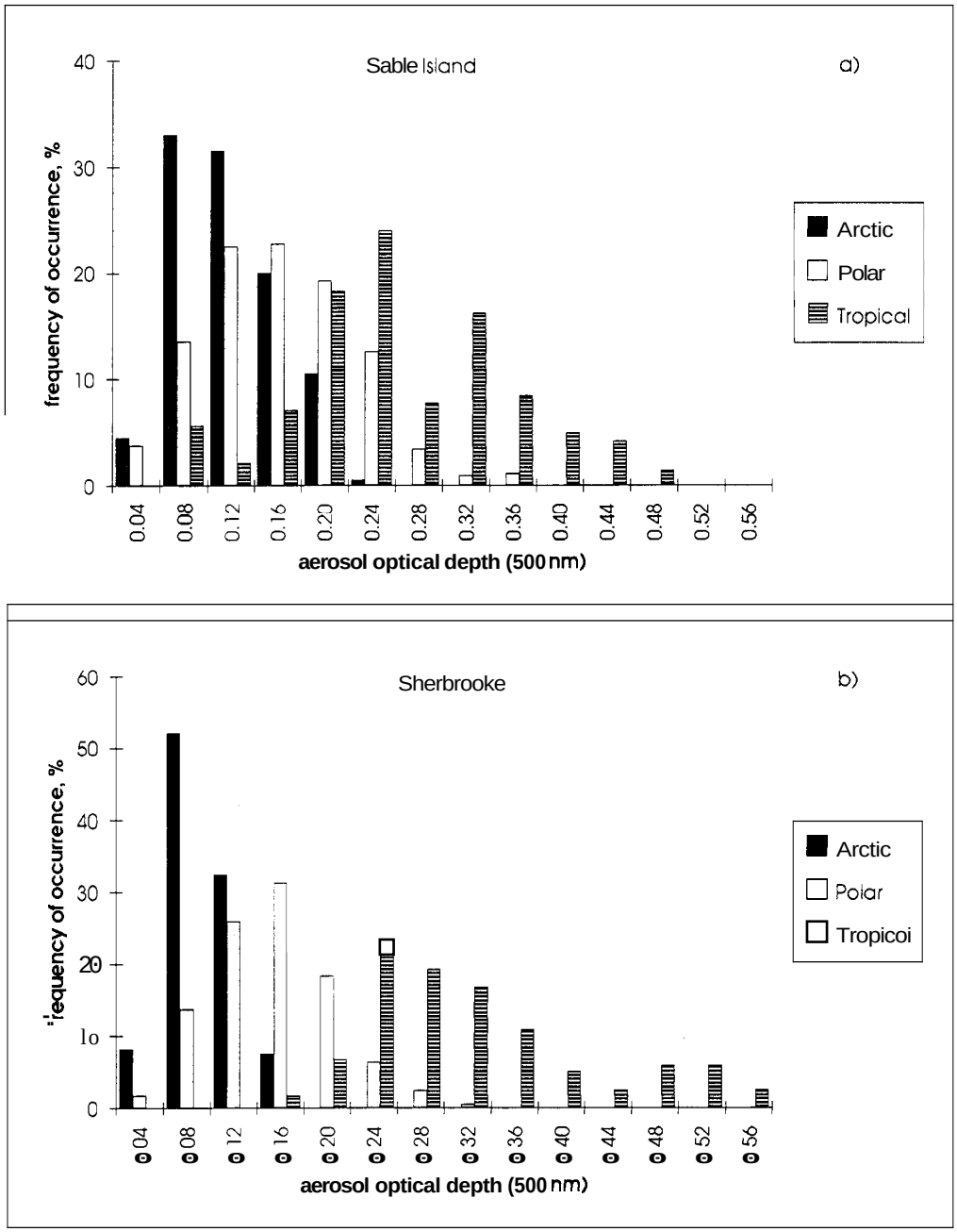


**Figure 8.** Frequency of occurrence of aerosol optical depth for the three principal air mass classes for (a) Sable Island, (b) Sherbrooke, (c) Wynyard, and (d) Cape St. James.

level of statistical detail which one can aspire to in the synoptical air mass analysis approach. The continental polar *air* mass data were subdivided into three source-tagged groups with southern, western, and northern continental labels. These results are notable since they enable us to subclassify the optical properties of continental polar air, the dominant air mass type for Sherbrooke.

**At** Wynyard the distribution of aerosol optical depth for polar air is very broad (Figure 8c). It is significantly different from **those** analyzed for Sable Island and Sherbrooke. **As** was pointed out above, polar air for Wynyard means Pacific air ***[Bryson,*** 19661. In the Pacific air observed at Wynyard, three subgroups were processed individually (Figure 9). "Pacific" designates air from the western sector, except the obvious chinook situations. The air arriving at Wynyard, with a strong westerly **flow** across the mountains and usually associated with a pronounced chinook event, is marked Pacific (chinook). The Pacific air crossing the mountains in Wyoming and reaching Wynyard from the southwest is marked Pacific southwest. Pacific (chinook) is characterized by a significantly lower $\tau_a$, whereas Pacific sw, compared to the Pacific grouping, is more turbid.

Air arriving at Wynyard from the northeastern sector (from Hudson Bay, for example) was considered as continental polar.

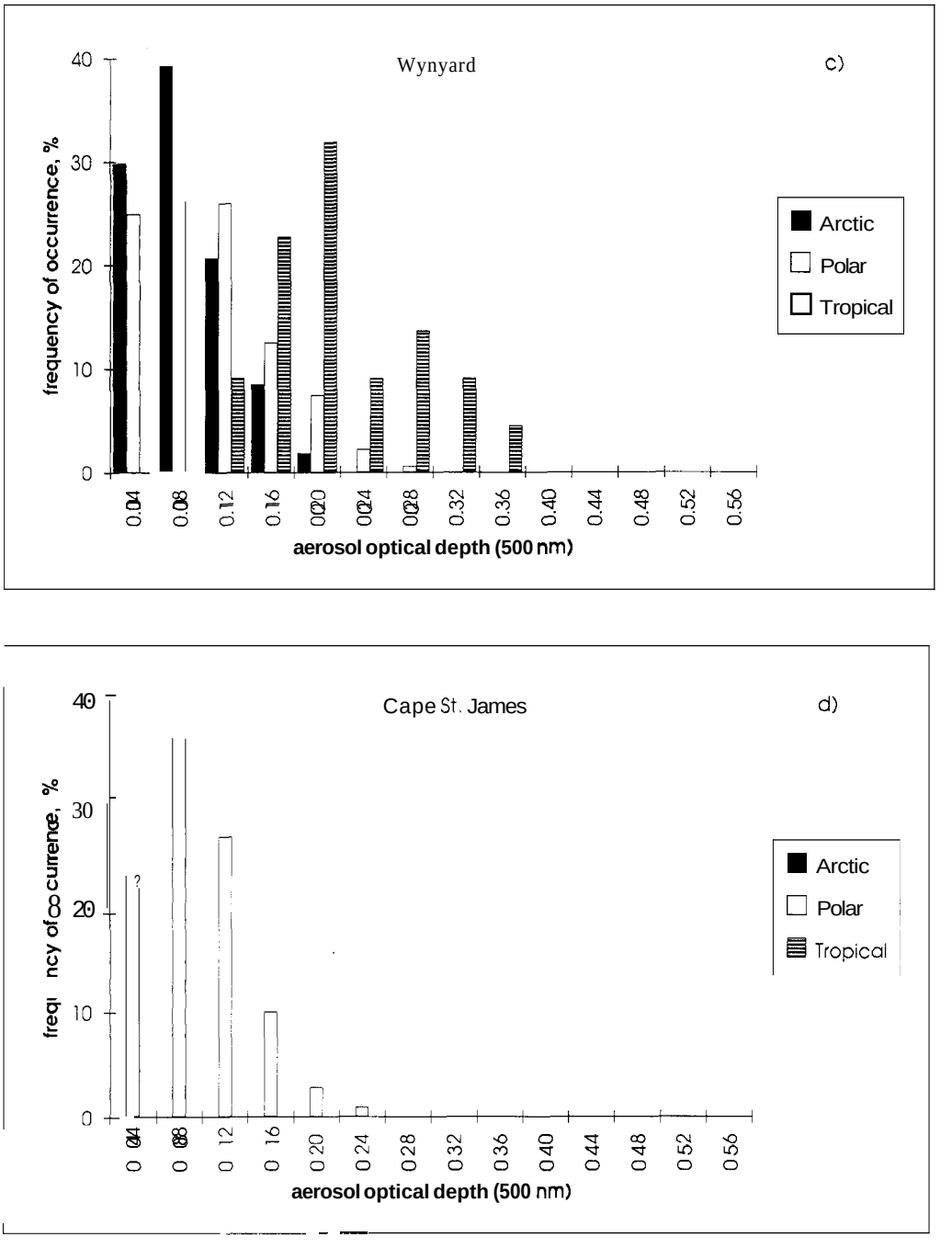


Figure 8. (continued)

Statistical characteristics for this air (see Table 5) are very close to the cPn type for Sherbrooke because the possibilities for modification are limited for air masses arriving from the northern sector.

Although tropical air is a rare occurrence at Wynyard, we have nonetheless presented results for this air mass type since its optical properties are substantially different. For Cape St. James the frequency distribution for polar air equivalent to maritime polar air with a certain amount of contamination. The distribution is narrow with 90% of the values less than 0.18.

### 5.1. Seasonal Trend of Aerosol Optical Depth for Arctic Air Masses

The gradual increase of $\tau_a$ during the winter months with a maximum in spring as well as a summer minimum was reported by *Shaw* [1982] for Alaska and by *Freund* [1983] for the Canadian Arctic and by ourselves for Sherbrooke [*Smirnov et al.*, 1994]. A similar seasonal trend of aerosol optical depth has been revealed for the three stations which experience Arctic air masses on a regular basis.

Mean monthly values of $\tau_a$ for Arctic air masses prior to the

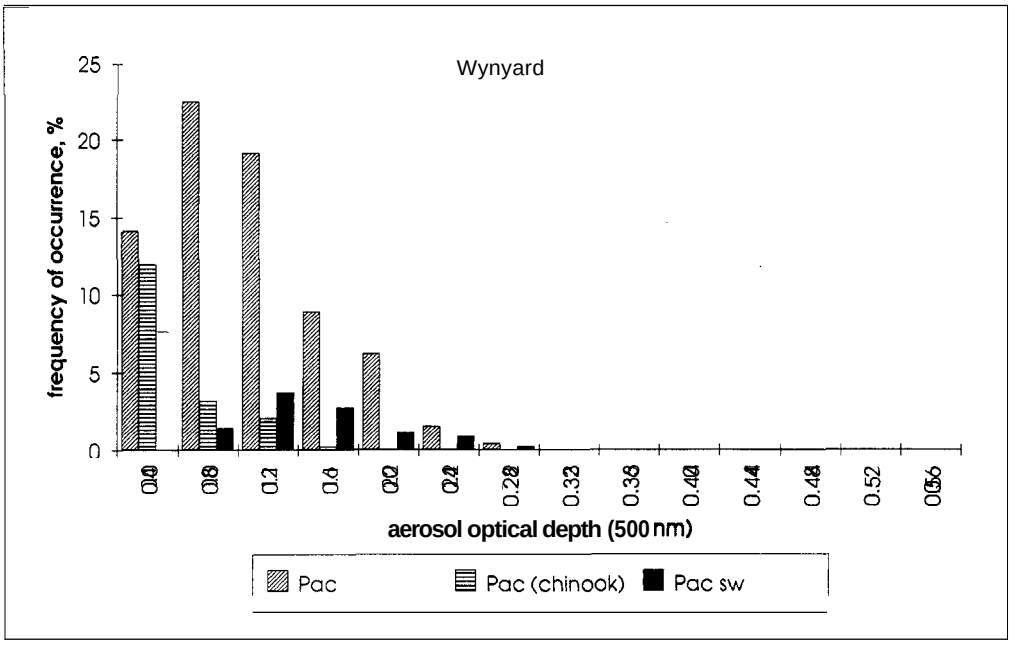


Figure 9. Frequency of occurrence of aerosol optical depth in maritime polar air mass for Wynyard. The sum of all frequences is equal to 100%. See Table 5 for the air mass codes.

Pinatubo eruption are presented in Figure 10. The pronounced maximum in the spring is evident especially for the Wynyard data. In this latter case the preservation of the Arctic air optical properties during passage from the Arctic regions is a likely reason for the feature being so much in evidence. The complex aerosol source history of air masses arriving at Sherbrooke and, especially, at Sable Island, obscures but does not mask the spring peak of $\tau_a$. The optical depth increase in the late fall for Sable Island is again probably influenced by the complex trajectories and varying aerosol contributions

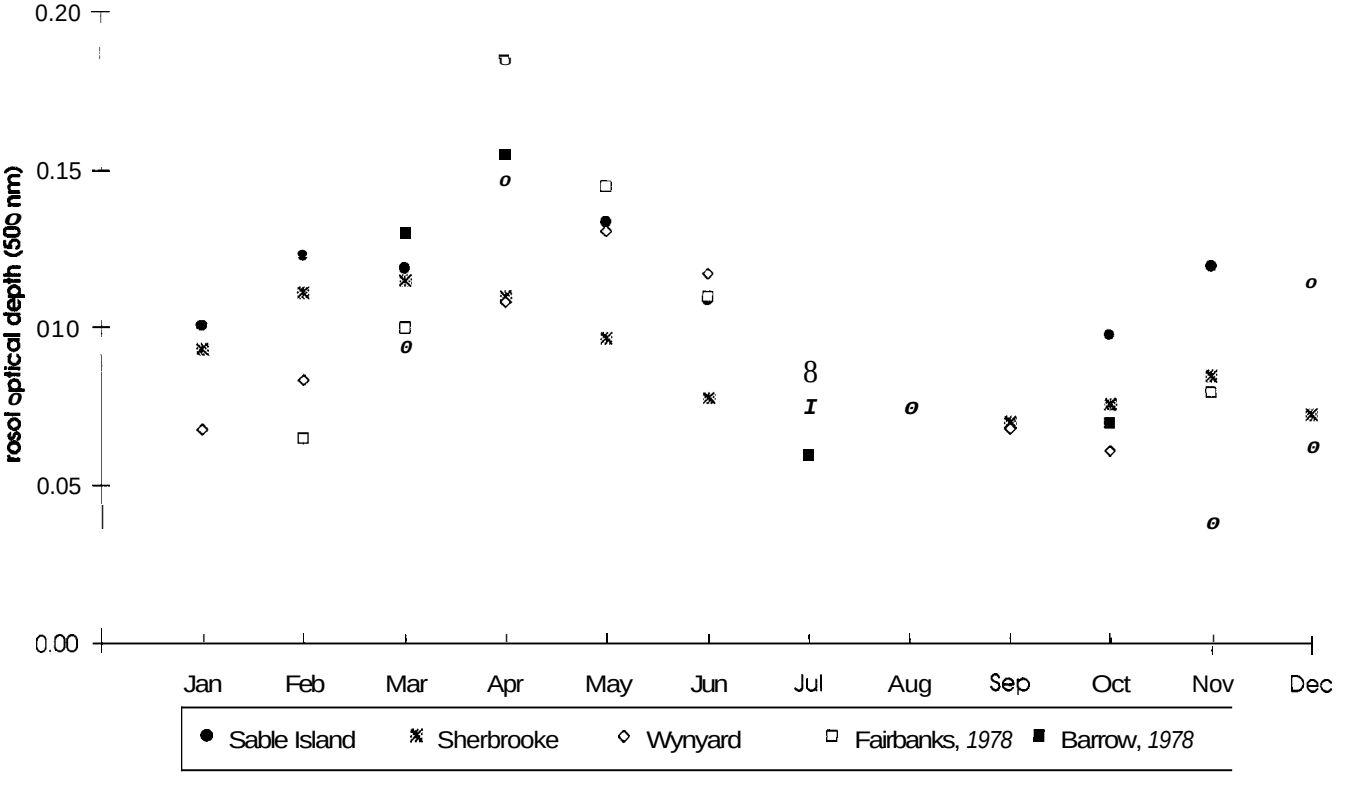


**Figure 10.** Variation of mean monthly values of aerosol optical depth in Arctic air mass for the three sunphotometer stations.

from regional sources. In Figure 10, mean $\tau_a$ values from Arctic stations in Alaska [*Shaw*, 1982] are also presented.

The general increase of aerosol concentration in the Arctic in winter and spring was also detected in ice cores from Greenland dated back to 18,000 B.C. [*Hammer*, 1978]. The natural seasonal variations of circulation patterns are thus likely to be the cause of this phenomenon. A stronger north-south air circulation in winter over North America induces a more active aerosol transport and increases the turbidity of Arctic air. In the warm season, zonal circulation patterns separate Arctic air from southern air sources and from aerosol contamination.

## 6. Conclusions

The principal conclusions drawn from our work can be summarized as follows:

1. Air mass relationships for the four stations sampled demonstrated the relevance of applying air mass classification criteria to the analysis and discrimination of atmospheric optical depth. Knowledge of the seasonal trend combined with information concerning air mass type would enable a coarse *a priori* estimation of aerosol optical depth in the absence of traditional optical data.

2. Synoptical air mass analysis facilitates the understanding of the mechanisms involved in the seasonal variations of aerosol optical depth and yields useful information about the atmospheric optical state.

3. The relevance of the synoptical air mass approach was in point of fact nicely demonstrated in one particular case: a seasonal aerosol optical depth trend for Arctic air masses was observed for the three sunphotometer stations which regularily experience this type of air mass.

4. The results of aerosol optical depth measurements acquired through the Canadian sunphotometer network showed significant differences between eastern and western Canadian stations.

5. The effect of the Pinatubo volcanic eruption was clearly seen in the measurements acquired at Sable Island, Nova Scotia.

With respect to the generality of the synoptical air mass analysis we can claim that similar air mass types are associated with similar optical depths (Table 5). However, the disparity between stations is sufficient enough that we must seek more detailed explanations of the source and trajectory flow mechanisms which affect air masses of the same type arriving at different sites.

Acknowledgments. The authors wish to acknowledge the financial support of the National Sciences and Engineering Research Council (NSERC) of Canada, the Atmospheric Environment Service (AES) of Environment Canada, and Fonds pour la Formation de Chercheurs et l'Aide à la Recherche (FCAR, Québec).

## References

Ahern, F. J., R.P. Gauthier, P.M. Teillet, J. Sirois, G. Fedosejevs, and D.Lorente, Investigations of continental aerosols with high-spectral-resolution solar-extinction measurements, *Appl. Opt*, 30, 5276-5287, 1991.

d'Almeida, G.A., P. Koepke, and E.P. Shettle, An approach to a global optical aerosol climatology, in *Aerosols and Climate*, edited by P.V.Hobbs and P.McCormick, pp.125-137, A.Deepak, Hampton, Va., 1988.

Bryson, R.A., Air masses streamlines and the boreal forest, *Geogr.* Bull., 8,228-269,1966.

Davies, J.A., R. Schroeder, and B. McArthur, Surface-based observations of volcanic aerosol effects, *Tellus, 40B*, 154-160, 1988.

Dutton, E.G., P. Reddy, S. Ryan, and J.J. DeLuisi, Features and effects of aerosol optical depth observed at Mauna Loa, Hawaii:1982-1992, *J. Geophys. Res.*, 99, 8295-8306, 1994.

Forgan, B.W. E.N. Rusina, J.J. DeLuisi, and B.B. Hicks, Measurements of atmospheric turbidity in BAPMON, and looking forward to GAW, *WMO Rep.*, draft 4, 80 pp., Geneva, 1993.

Freund, J., Aerosol optical depth in the Canadian arctic, *Atmos. Ocean, 21*, 158-167, 1983.

Halthore, R.N., B. Markham, R.A. Ferrare, and T.O. Aro, Aerosol optical properties over the midcontinental United States, *J. Geophys. Res.*, 97, 18,769-18,778, 1992.

Hammer, C.U., H.B. Clausen, W. Dansgaard, N. Gundestrup, S.J. Johnsen, and N. Rech, Dating of Greenland ice cores by flow models, isotopes, volcanic debris and continental dust, *J. Glaciol., 20*, 3-26, 1978.

Hay, J.E., and R.Darby, El Chichon - Influence on aerosol optical depth and direct, diffuse and total solar irradiances at Vancouver, B.C., *Atmos. Ocean.*, 22,354-368, 1984.

Iqbal, M., *An Introduction to Solar Radiation*, 390 pp., Academic, San Diego, Calif., 1983.

Kasten, F., A new table and approximation formula for the relative optical air mass, *Arch. Meteorol. Geophys. Bioklim., B14*, 206-233, 1966.

Kaufman, Y.J., and D. Tanré, Direct and indirect methods for correcting the aerosol effect on remote sensing, in *Physical Measurements and Signatures in Remote Sensing*, 6, 7-19, 1994.

Malm, W., and E.G. Walther, Reexamination of turbidity measurements near Page, Arizona, and Navajo generating station, *J. Appl. Meteorol., 18*, 953-955, 1979.

Michalsky, J.J., The astronomical almanac's algorithm for approximate solar position, *Sol. Energy, 40*, 227-235, 1988.

O'Neill, N.T., and J.R. Miller, Combined solar aureole and solar beam extinction measurements, 2; Studies of the inferred aerosol size distributions, *Appl. Opt.*. 23,3697-3704, 1984.

O'Neill, N.T., A. Royer, P. Cotb, and B. McArthur, Relations between optically derived aerosol parameters, humidity, and air-quality data in an urban atmosphere, *J. Appl. Meteorol., 32*, 1484-1498, 1993.

Penner, J.E., R.J. Charlson, J.M. Hales, N.S. Laulainen., R. Leifer, T. Novakov, J. Ogren, L.F. Radke, S.E. Schwartz, and L. Travis, Quantifying and minimizing uncertainty of climate forcing by anthropogenic aerosols, *Bull. Am. Meteorol. Soc., 75*, 375-400, 1994.

Peterson, J.T., E.C. Flowers, G.J. Berri, C.L. Reynolds, and J.H. Rudisill, Atmospheric turbidity over central North Carolina, *J. Appl. Meteorol., 20*, 229-241, 1981.

Polavarapu, R.J., Atmospheric turbidity over Canada, *J. Appl. Meteorol., 17*, 1368-1374, 1978.

Robinson, N., *Solar Radiation*, Elsevier, New York, 1966.

Russell, P.B., et al., Pinatubo and pre-Pinatubo optical depth spectra: Mauna Loa measurements, comparisons, inferred particle size distributions, radiative effects, and relationship to lidar data, *J. Geophys. Res.*, 98, 22,969-22,985, 1993.

Shaw, G.E., Atmospheric turbidity in the polar regions, *J. Appl. Meteorol.*, 21, 1080-1088, 1982.

Smimov, A., A. Royer, N.T. O'Neill, and A. Tarussov, A study of the link between synoptic air mass type and atmospheric optical parameters, *J. Geophys. Res.*, 99, 20,967-20,981, 1994.

Uboegbulam, T.C., and J.A. Davies, Turbidity in eastern Canada, *J. Clim. Appl. Meteorol.*, 22, 1384-1392,1983.

Valero, F.P.J., and P. Pilewskie, Latitudinal survey of spectral optical depths of the Pinatubo volcanic cloud-derived particle sizes, columnar mass loadings, and effects of planetary albedo, *Geophys. Res. Lett.*, 19,163-166, 1992.

Vigroux, E., Contribution a l'btude experimentale de l'absorption de l'ozone, *Ann. Phys.*, 8,709-762, 1953.

B.McArthur, Experimental Studies, Atmospheric Environment Service of Environment Canada, Downsview. Ontario, Canada.

N.T.O'Neill, A.Royer, A.Smirnov (corresponding author), and A.Tarussov, Centre d'Applications et de Recherches en Télédétection (CARTEL), Université de Sherbrooke, Sherbrooke, Québec, JIK 2R1, Canada.

('Received February 16, 1995; revised July 8, 1995;
accepted August 18, 1995.)